Regeneration, Reconstruction & Restoration
Original Article
Open Access

# Stress and Strain Distribution in the Reduced Periodontium of Canine Teeth: A Finite Element Analysis

**Soran Sijavandi[1] | Fazele Atarbashi-Moghadam[1, 2]* | Reza Amid[1, 2]**

1. Dental Research Center, Research Institute of Dental Sciences, Shahid Beheshti University of Medical Sciences, Tehran, Iran.
2. Department of Periodontics, Dental School of Shahid Beheshti University of Medical Sciences, Tehran, Iran.

**Article Info**

Received: 9 September, 2024

Accepted: 14 October, 2024

Published: 25 December, 2024

***Corresponding Author**

Fazele Atarbashi-Moghadam, Department of Periodontics, Dental School of Shahid Beheshti University of Medical Sciences, Tehran, Iran.

**Email:** dr.f.attarbashi@gmail.com

## Abstract

**Background and objectives:** Correct application of the Finite Element Method (FEM) can simulate tooth displacement and stress distribution in the periodontium under external forces and offer the correct prediction and appropriate therapeutical choices. The present study analyzed the alveolar bone's mechanical behavior under typical intrusion or oblique forces for several levels of reduced periodontium using a dynamic linear/nonlinear simulation.

**Materials and methods:** This study's modeling, meshing, simulation, and finite element analysis were carried out using SolidWorks software (2021, SP2, Dassault Systèmes). The mandibular and maxillary canines were modeled using cone beam computed tomography images. Teeth, lamina dura and cortical and cancellous bones were considered linear isotropic material, whereas the periodontal membrane was considered a hyper- elastic first-order Ogden material to account for its flexibility. Crown to root ratio (C/R) of 0.8, 1.25, 2 and 3.5 was simulated. All simulations were dynamic nonlinear/ linear to account for the natural displacements in the periodontium under occlusal forces. The teeth were submitted to intrusion or oblique (15 and 45 degrees) 100 Newton to simulate typical occlusal forces.

**Results:** The maximum von Mises stress and maximum equivalent strain for all models increase with bone loss. Furthermore, the rate at which these factors increase from each bone loss step to the following increases noticeably after 6 mm of bone loss. The amount and rate of increase in the maximum stress and stress experienced by alveolar bone are higher for forces with higher degrees of deviation from the tooth axis. The maximum stress and strain for the intrusion, 15-degree and 45-degree models were 137 Mpa/0.006, 268 Mpa/0.013 and 800 Mpa/0.040, respectively (All at C/R = 3.5).

**Conclusion:** Reduction of alveolar bone level (increased crown- to- root ratio) leads to higher levels of stress and strain, which show a steep rise at the 6 mm of bone loss. This observation leads our attention toward tooth-specific occlusal consideration in patients with reduced periodontium.

**Keywords:** Alveolar bone loss; Finite Element Analysis; Mechanical Stress; Periodontal ligament.

**Please cite this paper as:**

Sijavandi S, Atarbashi-Moghadam F, Amid R. Stress and Strain Distribution in the Reduced Periodontium of Canine Teeth: A Finite Element Analysis. Journal of “Regeneration, Reconstruction & Restoration” (Triple R). 2024; Volume 9: e15. Doi: 10.22037/rrr.v9.45531

## 1. Introduction

A reduced periodontium describes the reduction of load-bearing support of a tooth and apical displacement of its center of rotation. This phenomenon cannot be ignored while devising a treatment plan for periodontally treated teeth maintenance under occlusal or orthodontic forces (1). The Periodontal ligament or Periodontal Membrane

(PDM) is soft tissue full of blood vessels and connective tissue cells surrounding the tooth root (2). This tissue allows the stress from occlusal forces on the tooth to be appropriately distributed and absorbed by the alveolar bone (3). The stress distribution on the alveolar bone will change if the periodontium's geometry or quality changes (4). Any reduction in a tooth's periodontal support worsens its periodontal prognosis, making its clinical and radiographic evaluation necessary when deciding the tooth's fate (5). Such evaluation doesn't allow an in- depth assessment of stress distribution in the remaining periodontium, a task achievable using the Finite Element Method (FEM).

Biomechanical simulation of the periodontium requires appropriate modeling of several anatomic bodies while considering their nonhomogeneous- anisotropic behaviors. This task involves utilizing Cone Beam Computed Tomography (CBCT) images for the modeling and acquiring each material's mechanical behavior using experiments (6). In vivo experiments mostly measure the surface mechanical properties of biomaterial and human tissue. Still, understanding their internal mechanical behavior can be achieved using the FEM and visual presentations of various parameters at each point and surface (7). FEM is the only method that allows quantitative visualized stress distribution to be studied in a 3D object (8).

The FEM analysis of stress and strain distribution in the reduced periodontium under functional occlusal forces can help in prognosis determination and makes determining anatomical changes to the tooth to increase its prognosis possible (9).

Correct application of FEM can simulate tooth movement and stress distribution in the periodontium under external forces and offer the correct prediction and appropriate therapeutical choices. FEM studies for biomaterial and human tissues usually use static linear simulations. Still, a realistic situation involves dynamic nonlinear behaviors, especially in the case of PDM. Using nonlinear dynamic behavior in the PDM is the logical choice while studying human alveolar bone's stress or strain distribution and how it transfers the forces applied to the tooth to the alveolar bone (7). To the best of our knowledge, the present study is the first to evaluate different bone levels in reduced periodontium while considering PDM's nonlinear behavior. The present study analyzed the alveolar bone's mechanical behavior under typical occlusal intrusion or angeled forces for several levels of reduced periodontium using a dynamic linear/ nonlinear simulation.

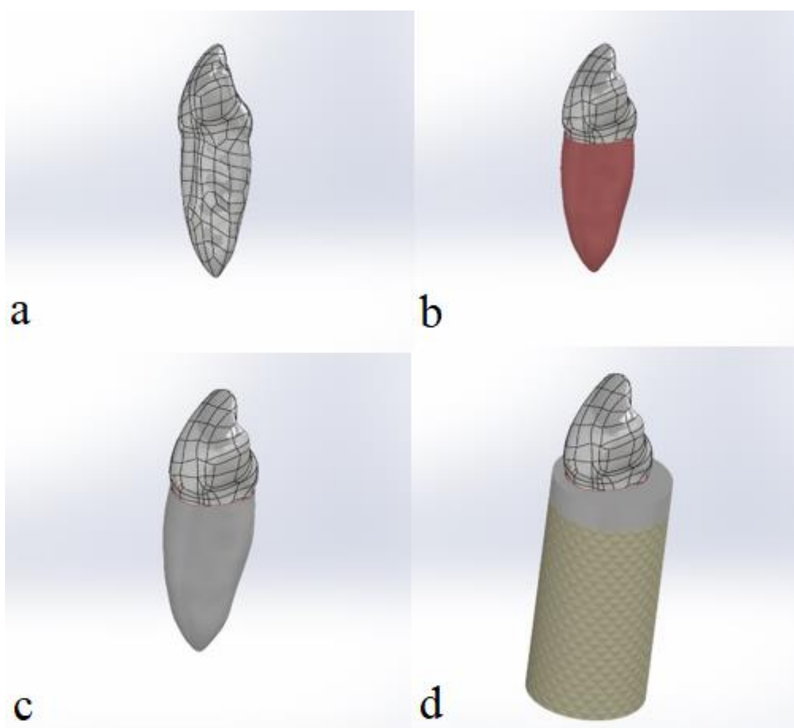


**Figure 1.** The 3D model created for the mandibular canine, including tooth (a), periodontal membrane (b), lamina dura (c), and bone (d).

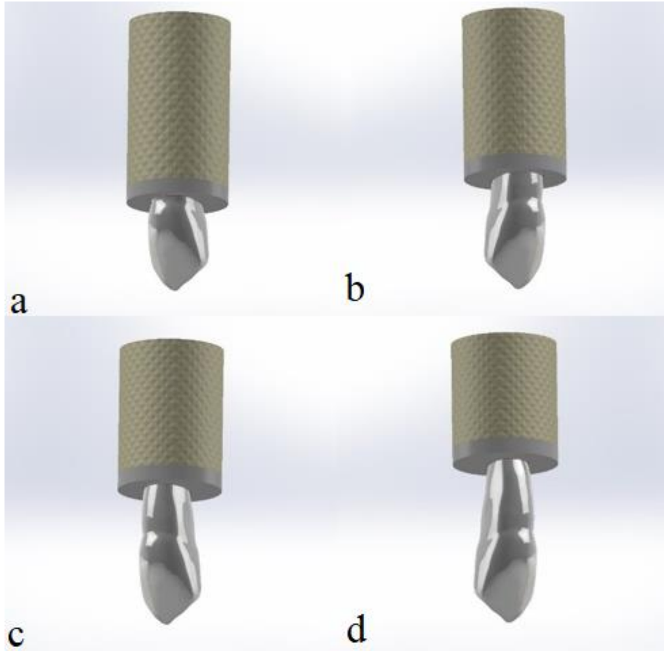


**Figure 2.** The 3D models with normal and reduced periodontium in the maxillary canine model; 0-mm bone loss (a), 3-mm bone loss (b), 6-mm bone loss (c), and 9-mm bone loss (d).

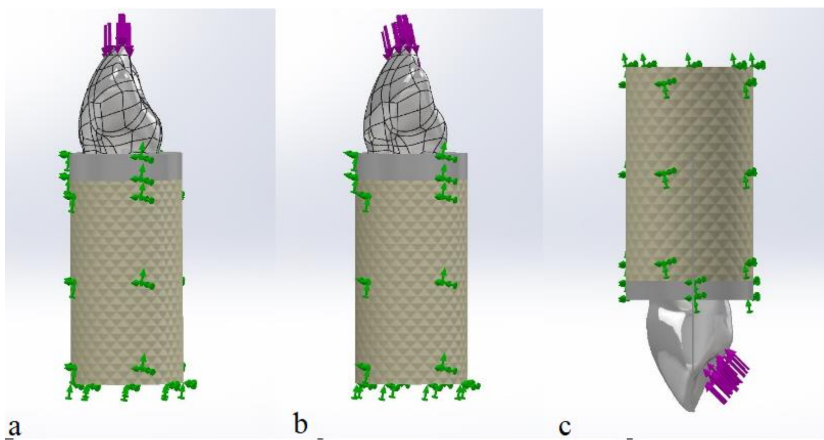


**Figure 3.** Applied force direction and boundary conditions on the normal models (no bone loss); Mandibular canine under intrusion force on the incisal edge (a), Mandibular canine under a 15-degree buccal force (b), and Maxillary canine under a 45-degree lingual force (c).

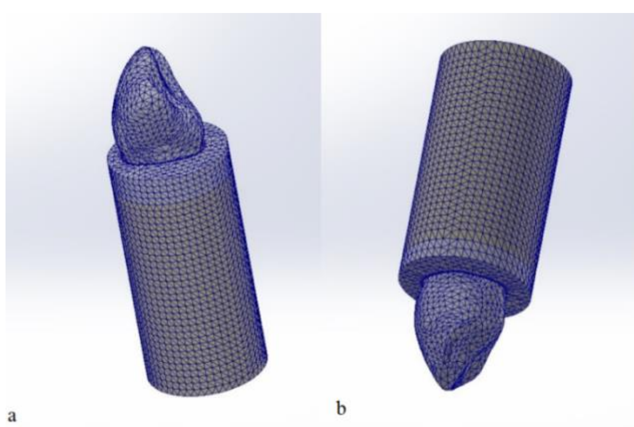


**Figure 4.** The meshed model for mandibular canine (a) and maxillary canine (b) with no bone loss.

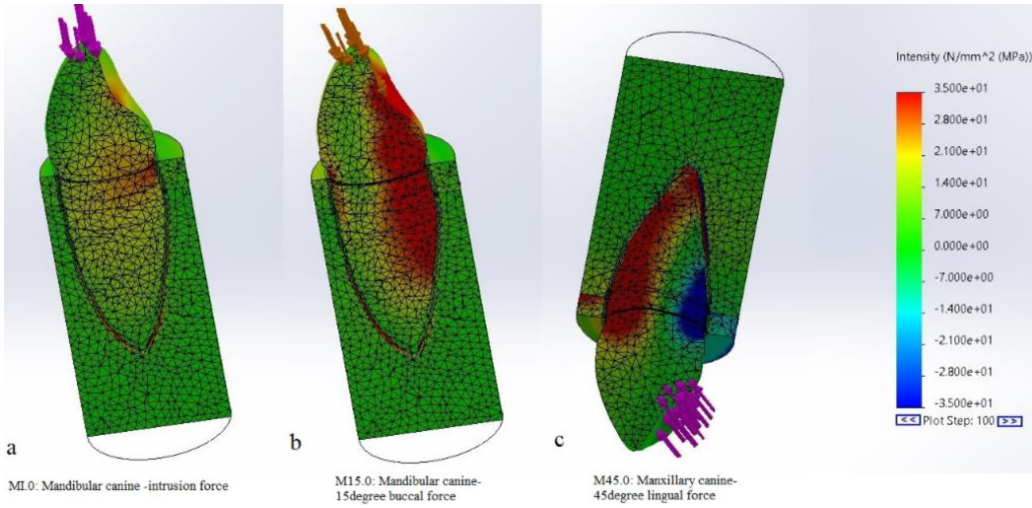


**Figure 5.** Stress intensity distribution for each primary model (MI.0 (a), M15.0 (b), and M45.0 (c)) at the final step of the simulation. (Tensile to compressive areas are visualized as a color spectrum from blue to red).

## 2. Materials and methods

### 2.1. Modeling

All modeling of this study was carried out using SolidWorks software (2021, SP2, Dassault Systèmes). The mandibular and maxillary canine teeth were modeled due to their critical functions in human occlusion, their long roots, and their essential role in controlling lateral movements of the jaw by guiding them in the vertical direction (10). Furthermore, their long roots make them a substantial abutment of choice for prosthetic treatments (10). Both teeth's basic geometry was extracted from the CBCT images of a healthy tooth using the method described by Sioustis et al. (8) and the Geomagic add-in package available for SolidWorks software (2021, SP2, Dassault Systèmes).

The surrounding bone, PDM, and alveolar bone proper (which is radiographically seen as lamina dura) were modeled and had 2mm of cortical bone at the crest level and a 0.2-0.5 mm thick lamina dura surrounding the tooth (11). The PDM's thickness varied from 0.2-0.4 mm around the tooth (11). In Reduced Periodontium (RP) models, the periodontium components had reduced heights (3, 6 and 9 millimeters of horizontal bone loss), however, were otherwise healthy to simulate a reduced periodontium after successful periodontal treatments meaning that even RP models had 2 mm of crest cortical bone. Figure 1 presents the modeled tooth, PDM, lamina dura and bone.

### 2.2. Applied forces and boundary conditions

The teeth were submitted to intrusion or oblique 100 Newton to simulate typical occlusal forces (12). The model's base (10 mm away from the root apex and the column surrounding the model were restricted from movement to simulate the stable position of the periodontium in the jaws (13). Three primary models were considered based on their tooth and force parameters; Figure 2 presents the 3D visualization of different heights of periodontium surrounding the tooth. Figure 3 shows the force and applied boundary conditions.

1. Model I (MI): Mandibular canine under 100N intrusion force at the incisal edge along the tooth axis. (MI.0, MI.3, MI.6 and MI.9 represent the reduced periodontium of 0, 3, 6 and 9 millimeters, respectively, or in the crown- to-root ratio of C/R = 0.8, 1.25, 2 and 3.5, respectively)
2. Model 15 (M15): Mandibular canine under a buccal force of 100 N applied on the incisal edge and a 15-degree angle with the tooth axis. (M15.0, M15.3, M15.6 and M15.9 represents the reduced periodontium of 0, 3, 6 and 9 millimeters, respectively, or in the crown- to- root ratio of C/R = 0.8, 1.25, 2 and 3.5, respectively)
3. Model 45 (M45): Maxillary canine under a lingual force of 100 N applied on the cingulum and a 45-degree angle with the tooth axis. (M45.0, M45.3, M45.6 and M45.9 represents the reduced periodontium of 0, 3, 6 and 9 millimeters, respectively, or in the crown- to- root ratio of C/R = 0.8, 1.25, 2 and 3.5, respectively)

### 2.3. Finite element analysis

All FEM analyses were carried out using the Solidworks Simulation Premium package available for SolidWorks software (2021, SP2, Dassault Systèmes). All materials but the PDM were considered linear isotropic. The mechanical properties of the PDM were inconsistent in the literature (14) and mainly were considered linear and did not account for its tightly confined yet flexible behavior; therefore, this study employed a model devised by Martinez et al. (15) for PDM as a hyperelastic first-order Ogden material which considers a first power material coefficient of $\alpha 1= 230$, first material constant of $\mu 1= 0.5e-4$ MPa and a Poisson's ratio of $\nu= 0.46$ (15). The mechanical properties acquired from similar studies for the material are presented in Table 1. The material was meshed using standard four-node pyramid or standard eight- node hexahedral elements with a minimum size of 0.04 mm and a maximum size of 0.8 mm. Perfect adhesion between different materials was modeled using bonded interaction surfaces considering node-to-node contact (Figure 4). The number of nodes and elements for the primary model without any bone loss (MI.0, M15.0 and M45.0) are presented in Table 2.

The simulation was considered a dynamic nonlinear one to account for the nonlinear behavior of the PDM and possible displacements in the geometry. Static stimulation is only applicable if the amount of strain is less than 0.4% which could be helpful under orthodontic force simulation or unrealistically small occlusion forces. However, a dynamic model applies the force in incremental steps and takes the new position of each component into account before moving to the next step (7).

## 3. Results

Von Mises stress distribution and equivalent stress distribution and their respective maximum and minimum points were extracted after simulation for the alveolar bone in each model. Von Mises stress and equivalent strain provide the stress and strain in each element with a directionless 3D mindset, and they do not represent compression or tension. Figure 5 illustrates the stress intensity distribution for each primary model at the final step of simulation to provide an understanding of tensile-compressive areas.

A buccolingual cut of von Mises stress distribution in the alveolar bone for all models with different bone levels is presented in Figure 6. This cut was chosen due to the forces applied in the buccolingual plane. The maximum and minimum von Mises stress in the alveolar bone and their area (Mesial, Distal, Buccal, Lingual- Apical third, Coronal third and mid- third of the tooth root) and the tensile or compressive nature obtained from the simulation are presented in Table 3.

A buccolingual cut of equivalent strain distribution in the alveolar bone for all models with different bone levels is presented in Figure 7. The maximum and minimum equivalent strain in the alveolar bone and their area (Mesial, Distal, Buccal, Lingual- Apical third, Coronal third and mid- third of the tooth root) and the tensile or compressive nature of the stress in the area obtained from the simulation are presented in table 4. Diagrams of maximum von Mises stress in the alveolar bone against the crown- to- root ratio are shown in Figure 8 and charts of maximum equivalent strain in the alveolar bone against the crown-to-root ratio are presented in Figure 9. As the bone level decreases (crown- to- root ratio increases), all models increase the maximum von Mises stress and maximum equivalent stress in the alveolar bone. The rate at which the maximum stress and maximum strain increase with bone loss shows different slopes between every two steps, and the slope becomes noticeably larger after the 6 mm bone loss step (Figure 8, 9). As the applied forces direction deviation further from the tooth axis, the observed increase in maximum stress and strain between consecutive steps becomes larger. The maximum von Mises stress from a C/R = 0.8 to 3.5 for the intrusion force, 15-degree force, and 45-degree force grows 2.53, 5.4 and 6.47-fold, respectively. The slope of the maximum von Mises stress diagram between the C/R= 2 to 3.5 while compared to its slope between C/R= 1.25 to 2 increases 0.85-1.52-fold. The maximum equivalent strain in the alveolar bone from a C/R= 0.8 to 3.5 for the intrusion force, 15-degree force and 45-degree force grows 2.62, 5.27, and 6.16 fold, respectively. The slope of the maximum equivalent diagram between the C/R= 2 to 3.5 while compared to its slope between C/R= 1.25 to 2 increases 0.86-4.58 fold.

## 4. Discussion

This study presented the mechanical behavior of alveolar bone surrounding human-canine teeth subjected to a typical intrusion and oblique mastication force of 100N for different levels of the reduced periodontium. The tooth, lamina dura, and cortical bones were considered linear isotropic material (15), which is appropriate due to their elastic macroscopic behavior under typical occlusal forces (13). The same cannot be considered for the PDM due to its flexible behavior (7). Dynamic simulations were used to analyze the models based on the changes in geometry, which is expected from the PDM (7). Few studies have considered dynamic models for orthodontic forces (16-18) but not under typical occlusal forces.

The teeth and surrounding periodontium could be subjected to a range of forces from 0 to 500N during normal mastication (19), however, the PDM structure allows for proper stress distribution; therefore, this heavy load doesn't lead to any trauma in the healthy and normal periodontium. The periodontium can change due to periodontal disease; if noticeable bone loss happens, treatment of the periodontal disease leads to "reduced periodontium," a situation in which, although the disease is treated, the level of alveolar bone, lamina dura, and PDM have decreased (19, 20).

The lamina dura is a radiographic term describing the alveolar bone proper, which covers the teeth's socket wall; therefore, any displacement in the tooth and the PDM face

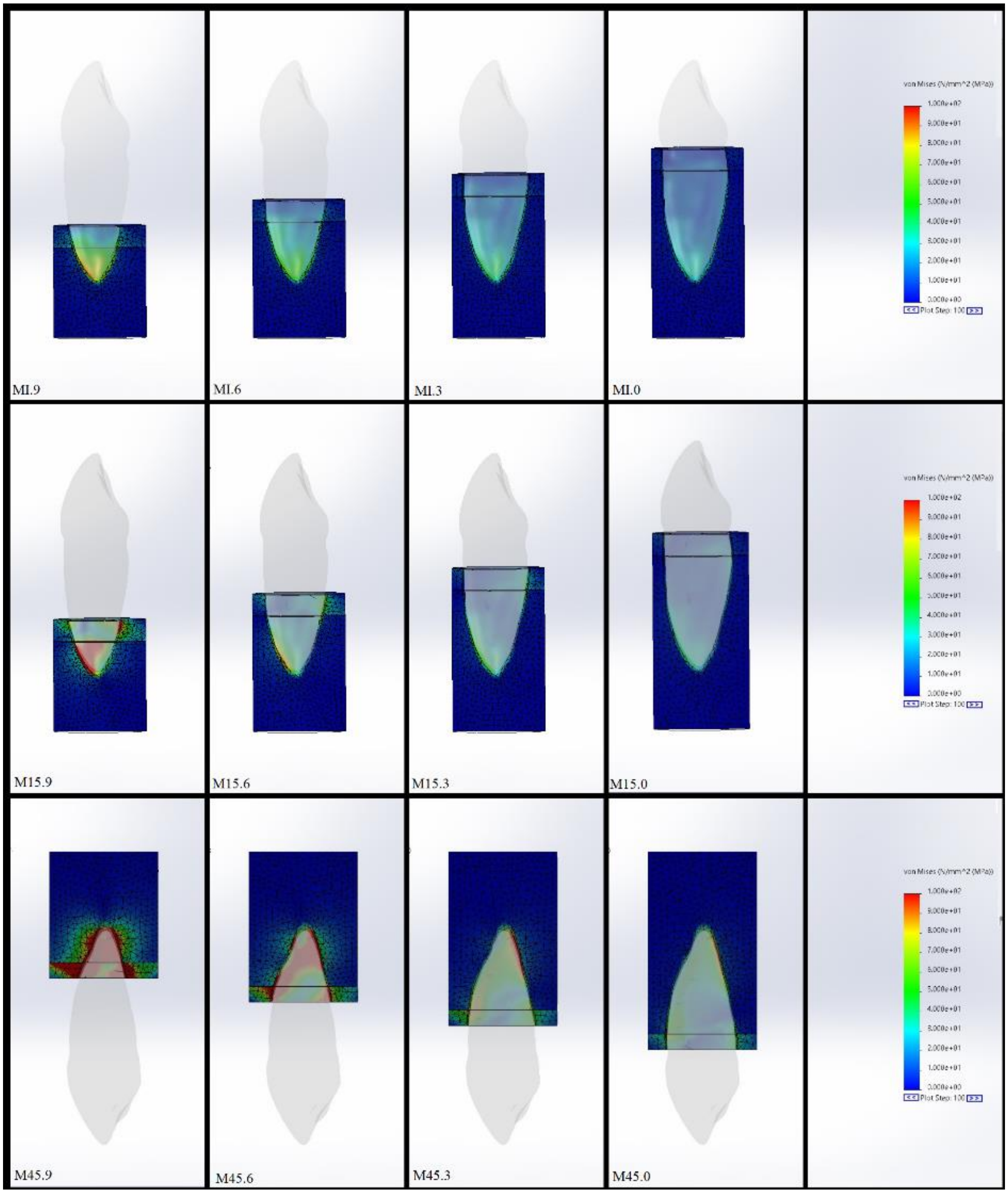


**Figure 6.** Buccolingual cut of von Mises stress distribution in the alveolar bone for all models with different bone levels. In each name, (*.#) * refers to the primary model, and # refers to bone level: MI. #: Mandibular canine under 100N intrusion force at the incisal edge along the tooth axis, M15. #: Mandibular canine under a buccal force of 100 N applied on the incisal edge and a 15-degree angle with the tooth axis, M45. #: Maxillary canine under a lingual force of 100 N applied on the cingulum and a 45-degree angle with the tooth axis. *.0, *.3, *.6 and *.9 represent the reduced periodontium of 0, 3, 6 and 9 millimeters, respectively.

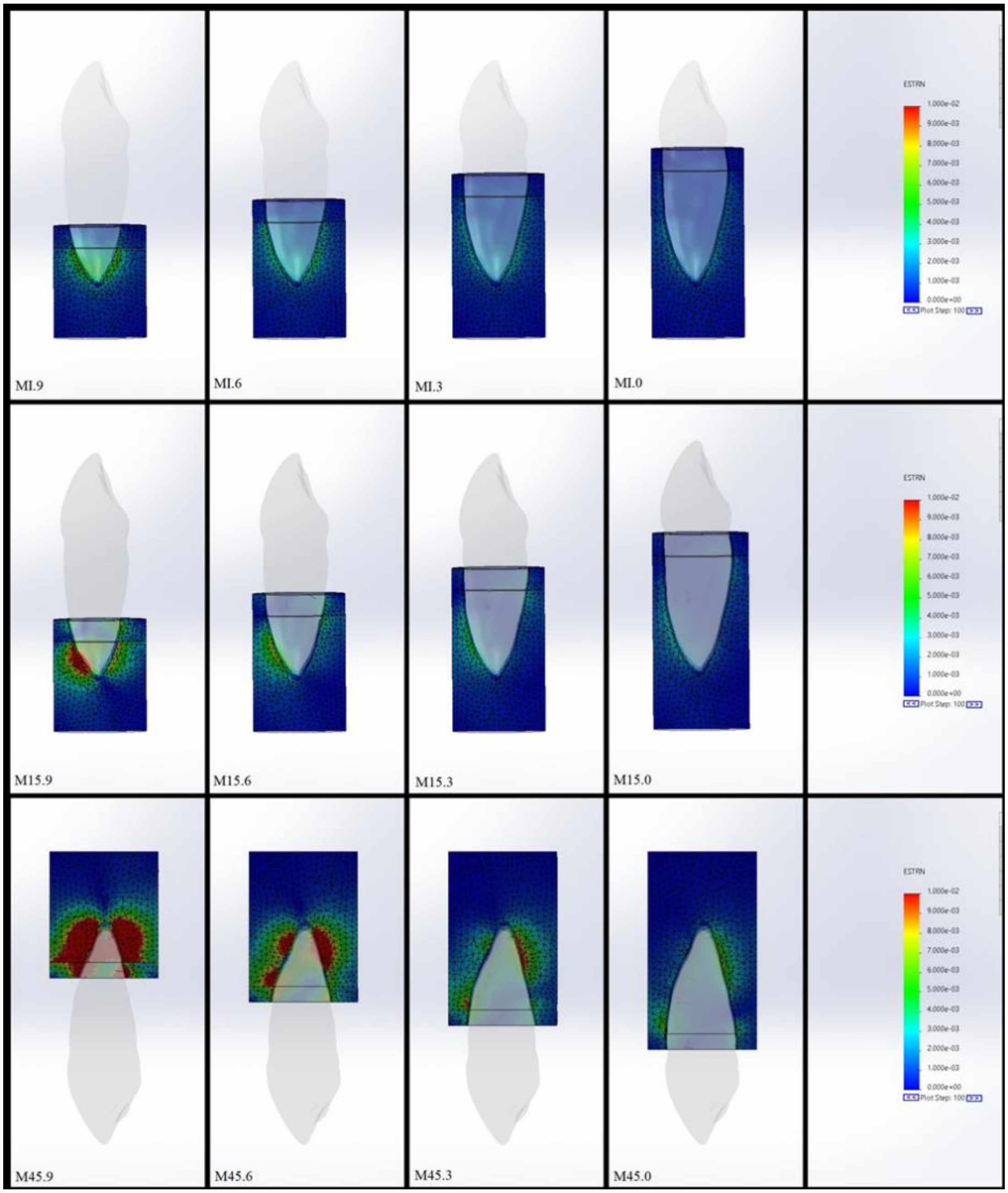


**Figure 7.** Buccolingual cut of equivalent strain distribution in the alveolar bone for all models with different bone levels. In each name, (*.#) * refers to the primary model, and # refers to bone level: MI. #: Mandibular canine under 100N intrusion force at the incisal edge along the tooth axis, M15. #: Mandibular canine under a buccal force of 100 N applied on the incisal edge and a 15-degree angle with the tooth axis, M45. #: Maxillary canine under a lingual force of 100 N applied on the cingulum and a 45-degree angle with the tooth axis. *.0, *.3, *.6 and *.9 represent the reduced periodontium of 0, 3, 6 and 9 millimeters, respectively.

**Table 1.** The mechanical properties acquired from similar studies for the material. (E= Young's modulus, α1= first power material coefficient, μ1= first material constant and ν= Poisson's ratio).

| Material | Material law | Parameters |
|---|---|---|
| **Tooth (22)** | Linear elastic | E= 20,300N/mm$^2$, ν= 0.3 |
| **Lamina dura (40, 41)** | Linear elastic | E=13,700 N/mm$^2$, ν= 0.3 |
| **PDM (17)** | Hyper elastic first-order Ogden | $\mu_1$= 0.5 × 10−4 MPa, α1= 230, ν= 0.46 |
| **Cortical bone (40, 14)** | Linear elastic | E= 13,700N/mm$^2$, ν= 0.3 |
| **Cancellous bone (17)** | Linear elastic | E= 2,000 N/mm$^2$, ν= 0.31 |

**Table 2.** The number of nodes and elements for the primary model without any bone loss (MI.0, M15.0 and M45.0)

| Component | Maxillary canine (M45.0) | | Mandibular canine (MI.0 and M15.0) | |
|---|---|---|---|---|
| | Elements | Nodes | Elements | Nodes |
| **Tooth** | 15894 | 76142 | 16973 | 77312 |
| **Lamina dura** | 4804 | 9623 | 4924 | 9946 |
| **PDM** | 4458 | 8997 | 4622 | 9315 |
| **Cortical bone** | 3383 | 5830 | 4268 | 7110 |
| **Cancellous bone** | 43969 | 63673 | 37386 | 54926 |
| **Whole model** | 72508 | 164265 | 68713 | 158609 |

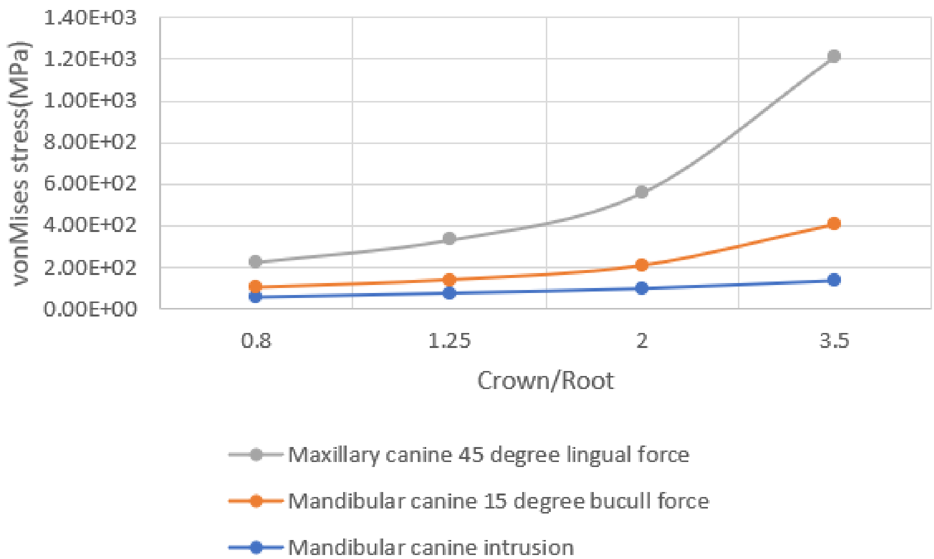


**Figure 8.** Diagrams of maximum von Mises stress in the alveolar bone against the crown to root ratio for all models under 100N force.

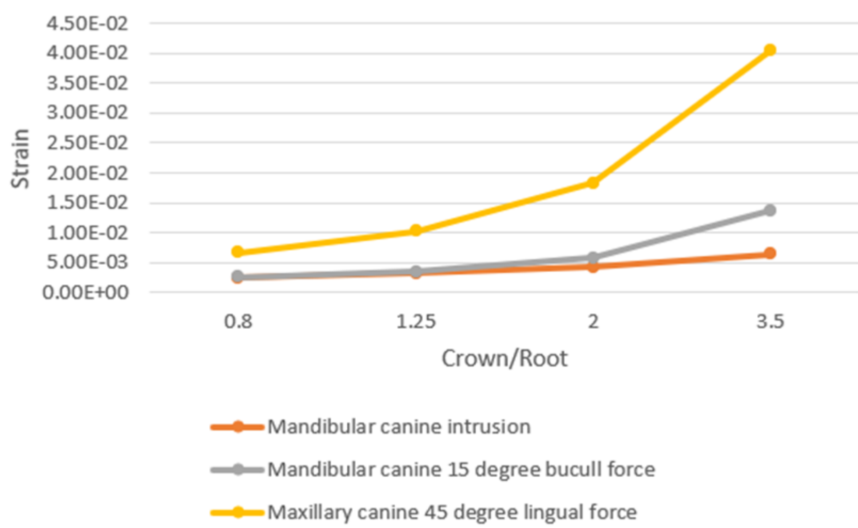


**Figure 9.** Diagrams of maximum equivalent strain in the alveolar bone against the crown to root ratio for all models under 100N force.

**Table 3.** Maximum and minimum von Mises stress in the alveolar bone and their area (Mesial, Distal, Buccal, Lingual- Apical third, Coronal third, mid- third of the tooth root) and the tensile or compressive nature obtained from the simulation (C/R= Crown to Root ratio).

| Model No. | Bone Loss (mm) | C/R | Maximum | | | | Minimum | | | |
|---|---|---|---|---|---|---|---|---|---|---|
| | | | Von Mises (Mpa) | Shear (Mpa) | Nature | Area | Von Mises (MPa) | Shear (MPa) | Nature | Nature |
| | | | **Mandibular canine under 100N intrusion force at the incisal edge along the tooth axis.** | | | | | | | |
| **MI.0** | 0 | 0.8 | 5.40E+01 | 1.77E+01 | Compressive | Apical Lingual | 7.26E-01 | -2.39E+01 | Tensile | Coronal Buccal |
| **MI.3** | 3 | 1.25 | 7.46E+01 | 2.24E+01 | Compressive | Apical Lingual | 1.61E+00 | -3.07E+01 | Tensile | Coronal Buccal |
| **MI.6** | 6 | 2 | 9.75E+01 | 2.99E+01 | Compressive | Apical Lingual | 1.94E+00 | -4.13E+01 | Tensile | Coronal Lingual |
| **MI.9** | 9 | 3.5 | 1.37E+02 | 4.87E+01 | Compressive | Apical Lingual | 2.30E+00 | -6.11E+01 | Tensile | Coronal Buccal |
| | | | **Mandibular canine under a buccal force of 100N applied on the incisal edge and a 15-degree angle with the tooth axis.** | | | | | | | |
| **MI.0** | 0 | 0.8 | 4.96E+01 | 1.67E+01 | Compressive | Apical Buccal | 9.66E-01 | -2.00E+01 | Tensile | Root- tip |
| **MI.3** | 3 | 1.25 | 6.52E+01 | 2.11E+01 | Compressive | Apical Buccal | 1.49E+00 | -2.75E+01 | Tensile | Root- tip |
| **MI.6** | 6 | 2 | 1.11E+02 | 3.21E+01 | Compressive | Apical Buccal | 1.80E+00 | -4.52E+01 | Tensile | Root- tip |
| **MI.9** | 9 | 3.5 | 2.68E+02 | 7.57E+01 | Compressive | Apical Buccal | 3.37E+00 | -1.05E+02 | Tensile | Root- tip |
| | | | **Maxillary canine under a lingual force of 100N applied on the cingulum and a 45-degree angle with the tooth axis.** | | | | | | | |
| **MI.0** | 0 | 0.8 | 1.24E+02 | 3.06E+01 | Compressive | Apical Lingual | 2.04E+01 | -6.21E+01 | Compressive | Root- tip |
| **MI.3** | 3 | 1.25 | 1.24E+02 | 3.67E+01 | Compressive | Apical Lingual | 4.70E+00 | -9.87E+01 | Compressive | Root- tip |
| **MI.6** | 6 | 2 | 1.24E+02 | 7.77E+01 | Compressive | Apical Lingual | 6.01E+00 | -1.85E+02 | Compressive | Root- tip |
| **MI.9** | 9 | 3.5 | 8.03E+02 | 2.54E+02 | Compressive | Apical Lingual | 1.97E+01 | -4.45E+02 | Compressive | Coronal Distal |

**Table 4.** Maximum and minimum equivalent strain in the alveolar bone and their area (Mesial, Distal, Buccal, Lingual- Apical third, Coronal third, mid- third of the tooth root) and the tensile or compressive nature of the stress in the area obtained from the simulation (C/R= Crown length to Root length ratio).

| Model No. | Bone Loss (mm) | C/R | Maximum | | | Minimum | | |
|---|---|---|---|---|---|---|---|---|
| | | | Strain | Stress Nature | Area | Strain | Stress Nature | Area |
| | | | **Mandibular canine under 100N intrusion force at the incisal edge along the tooth axis.** | | | | | |
| **MI.0** | 0 | 0.8 | 2.45E-03 | Compressive | Apical Lingual | 6.28E-05 | Tensile | Coronal Buccal |

| | | | | | | | | |
|---|---|---|---|---|---|---|---|---|
| **MI.3** | 3 | 1.25 | 3.17E-03 | Compressive | Apical Lingual | 4.50E-05 | Tensile | Coronal Lingual |
| **MI.6** | 6 | 2 | 4.16E-03 | Compressive | Apical Lingual | 1.94E-04 | Tensile | Coronal Lingual |
| **MI.9** | 9 | 3.5 | 6.42E-03 | Compressive | Apical Lingual | 1.17E-04 | Tensile | Coronal Buccal |
| **Mandibular canine under a buccal force of 100N applied on the incisal edge and a 15-degree angle with the tooth axis.** | | | | | | | | |
| **MI.0** | 0 | 0.8 | 2.58E-03 | Compressive | Apical Distal | 1.34E-04 | Tensile | Coronal Mesial |
| **MI.3** | 3 | 1.25 | 3.44E-03 | Compressive | Apical Distal | 1.68E-04 | Tensile | Coronal Mesial |
| **MI.6** | 6 | 2 | 5.73E-03 | Compressive | Apical Distal | 3.01E-04 | Tensile | Mid Lingual |
| **MI.9** | 9 | 3.5 | 1.36E-02 | Compressive | Apical Distal | 3.25E-04 | Tensile | Coronal Mesial |
| **Maxillary canine under a lingual force of 100N applied on the cingulum and a 45-degree angle with the tooth axis.** | | | | | | | | |
| **MI.0** | 0 | 0.8 | 6.57E-03 | Compressive | Apical Lingual | 2.33E-04 | Compressive | Coronal Distal |
| **MI.3** | 3 | 1.25 | 1.02E-02 | Compressive | Apical Lingual | 3.75E-04 | Compressive | Coronal Distal |
| **MI.6** | 6 | 2 | 1.83E-02 | Compressive | Apical Lingual | 7.06E-04 | Compressive | Coronal Distal |
| **MI.9** | 9 | 3.5 | 4.05E-02 | Compressive | Apical Lingual | 1.26E-03 | Compressive | Coronal Distal |

the lamina dura as a barrier before affecting the cancellous bone, a notion completely ignored by most finite element studies concerning teeth (21-25). Modeling the lamina dura as a thin yet resilient layer, as was modeled in this study, allows the simulation of teeth to be closer to reality.

As the bone level in the reduced periodontium decreases, the maximum von Mises stress, shear stress, and maximum equivalent strain in the alveolar bone increases for all models, an expected result that is in unity with the literature (23, 25-29). The maximum von Mises stress in the alveolar bone for 3 to 9 mm reduction in the periodontium grows 2.53, 5.4, and 6.47-fold the intrusion force, 15-degree force, and 45-degree force, respectively. Such an increase in the amount of bone stress results from reduced supporting tissue to bear the force. Furthermore, as the bone level decreases, the tooth's center of rotation is displaced further apically, allowing the force to act with higher momentum, leading to increased stress and strain in the alveolar bone (23, 30). Agarwal et al. (25) reported a 1.7-fold increase in stress between 0 to 8 mm horizontal bone loss for intrusion forces. Our results show a 1.81-fold increase in maximum stress between 0-6 mm in the reduced periodontium and a 2.53-fold increase between 0-9mm in the case of intrusion forces. Geramy et al. (20) reported the same pattern of stress increase in horizontal bone loss, but the level of stress in their model raised 9.9 fold for 0 to 8 mm of stress. The pattern of stress change in these studies is congruent with our research. The increase in stress is close to the results presented by Agarwal et al. (25). But the 9.9-fold increase mentioned by Geramy et al. (20) is much higher than our results for intrusion forces, which is due to the absence of lamina dura in their model and the fact that they have only considered cortical crestal bones for healthy periodontium with normal bone height, an assumption only valid for persistent periodontal disease.

The rate at which the maximum stress and maximum strain increase with bone loss show different slopes between every two steps, an observation most visible after

6 mm bone loss. This phenomenon can be due to the increasing tipping ability of the force as a result of less support tissue. However, the ability of functional forces to tip the tooth does not lead to notable changes in small reductions of the periodontium. As the reduction continues, the lower center of rotation strengthens the same force's ability to cause stress and strain in the alveolar bone (20). This pattern of steeper stress and strain change at the level of 6mm bone loss was also present in Geramy et al. results (20, 28), although they noted another such slope change at the 2.5 mm of bone loss, representing the end of crestal cortical bone. Although not quantified in our analysis, this change isn't expected to happen in reduced periodontium due to the presence of crestal cortical bone in all simulation steps of bone loss.

As per visualizations presented in Figures 6-7, the strain and stress experience a drop while transitioning from cortical to cancellous bones. Such a drop results from the much higher elastic modulus of the cortical bone compared to the cancellous bone, which reduces stress and strains in the cancellous bone, especially in areas closer to the crestal cortical bone (28). Such a drop will only occur if the periodontium is considered reduced yet healthy; therefore, such similar patterns can only be seen at the 0mm bone loss in other studies (18, 20, 25, 28)

The maximum stress and strain in the alveolar bone in all models are in the apical area and result from compressive stresses. The maximum stress and strain for intrusion and oblique lingual forces happened on the lingual side, while the oblique buccal load led to a maximum stress area on the buccal side. These results are congruent with Geramy et al.'s results (20, 28), but other studies (18, 31) report the highest stress and strains positioned at the crestal level, which is a direct result of not differentiating between lamina dura, cortical and crestal bones which could be accepted in cases other than healthy reduced periodontium.

With the loss of bone height due to periodontal disease, a question arises: Can the changed periodontium bear the same typical occlusal forces as a normal healthy periodontium? This question remains valid even after periodontal treatment in cases of healthy reduced periodontium. Animal studies have proven that reduced periodontium can lead to faster bone loss, even at typical occlusal forces (32-35).

The results of strain analysis presented in Table 4 show that the strain level can be higher with more bone loss. In such high crown- to- root ratios, the typical occlusal force can lead to secondary trauma from occlusion, especially in oblique forces (20, 28). The possibility of typical occlusal forces changing into traumatic forces in cases of reduced periodontium should be considered in occlusal therapies, which can lead to a higher prognosis and higher success rate for regenerative and maintenance periodontal treatments (28, 36). The recommended crown-to-root ratio for a tooth to be a reliable abutment for fixed prosthetic crowns is between 0.6 to 1 (37), which is below the C/R= 1.25, at which our study starts to show a notable increase in maximum stress and strain. Still, it should be noted that the 0.6 to 1 recommended level is for a crown that might withstand higher occlusal forces than the typical 100N considered for this study. Crown- to- root ratios greater than one has been deemed acceptable to forces up to 260 N (37).

The main limitation of this study is the same as other studies, which is not being able to model each element as non- homogeneous anisotropic entities with different modules and coefficients based on the direction of displacement in the nodes. Such a limitation is most likely to be resolved in the future using the increased computational power of computers. Further studies concerning teeth other than the canines with a higher number of reduction steps are recommended.

## 5. Limitations

During the chewing process, jaw movements apply forces at different angles to the teeth, however, our study limited to model only 3 types of forces.

## 6. Conclusion

Reduction of alveolar bone level (increased crown- to-root ratio) leads to higher levels of stress and strain, which show a steep rise at the 6 mm of bone loss. This observation leads our attention toward tooth- specific occlusal consideration in patients with reduced periodontium.

## Acknowledgements

None.

## Ethics

The study was approved by the Ethics Committee of Shahid Beheshti University of Medical Sciences (IR.SBMU.DCR.REC.1399.086).

## Author contributions

Soran Sijanivandi: Conceptualization, Methodology, Investigation, Statistical analysis, Writing - Original draft,

Writing - Review & editing.
Fazelel Atarbashi-Moghadam: Conceptualization, Supervision, Methodology, Investigation, Writing- Original draft, Writing- Review & editing.
Reza Amid: Conceptualization, Supervision, Methodology, Investigation, Writing- Review & editing.

## Conflict of interest

The authors declare no conflict of interest.

## Funding

None.

## References


1. Gkantidis N, Christou P, Topouzelis N. The orthodontic-periodontic interrelationship in integrated treatment challenges: a systematic review. J Oral Rehabil. 2010;37(5):377-90.
2. Ohshima J, Abe S, Morita M, Tanaka N, Yamaguchi M, Hayashi M. Time-course study of genetic changes in periodontal ligament regeneration after tooth replantation in a mouse model. Sci Rep. 2024 Jul 5;14(1):15502. doi: 10.1038/s41598-024-66542-8. PMID: 38969768; PMCID: PMC11226448.
3. Ortún-Terrazas J, Cegoñino J, Pérez Del Palomar A. In silico study of cuspid' periodontal ligament damage under parafunctional and traumatic conditions of whole-mouth occlusions. A patient-specific evaluation. Comput Methods Programs Biomed. 2020 Feb;184:105107. doi: 10.1016/j.cmpb.2019.105107. Epub 2019 Oct 4. PMID: 31629157.
4. Poiate IA, de Vasconcellos AB, de Santana RB, Poiate E. Three-dimensional stress distribution in the human periodontal ligament in masticatory, parafunctional, and trauma loads: finite element analysis. J Periodontol. 2009;80(11):1859-67.
5. Moser P, Hammerle CH, Lang NP, Schlegel-Bregenzer B, Persson R. Maintenance of periodontal attachment levels in prosthetically treated patients with gingivitis or moderate chronic periodontitis 5-17 years post therapy. J Clin Periodontol. 2002;29(6):531-9.
6. Kober C, Stubinger S, Hellmich C, Sader R, Zeilhofer HF. Finite element simulation of the human mandible: the role of (natural) teeth. Int J Comput Dent. 2008;11(3-4):169-74.
7. Wakabayashi N, Ona M, Suzuki T, Igarashi Y. Nonlinear finite element analyses: advances and challenges in dental applications. J Dent. 2008;36(7):463-71.
8. Sioustis I-A, Axinte M, Prelipceanu M, Martu A, Kappenberg-Nitescu D-C, Teslaru S, et al. Finite Element Analysis of Mandibular Anterior Teeth with Healthy, but Reduced Periodontium. Applied Sciences. 2021;11(9):3824.
9. Kawarizadeh A, Bourauel C, Zhang D, Gotz W, Jager A. Correlation of stress and strain profiles and the distribution of osteoclastic cells induced by orthodontic loading in rat. Eur J Oral Sci. 2004;112(2):140-7.
10. Neeta Pasricha VS, Satpreet Bhasin, Monika Makkar. Canine protected occlusion.]ndian Journal of Oral Sciences. 2012;3(1):13-8.
11. Kurniawan D, Nor FM, Lee HY, Lim JY. Finite element analysis of bone-implant biomechanics: refinement through featuring various osseointegration conditions. Int J Oral Maxillofac Surg. 2012;41(9):1090-6.
12. Bakhit M, Okada D, Luo S, Shin C, Ogura R, Komada W, et al., editors. The stress distribution within dentin upon the use of different restoration materials2017.
13. Azcarate-Velazquez F, Castillo-Oyague R, Oliveros-Lopez LG, Torres-Lagares D, Martinez-Gonzalez AJ, Perez-Velasco A, et al. Influence of bone quality on the mechanical interaction between implant and bone: A finite element analysis. J Dent. 2019;88:103161.
14. Fill TS, Toogood RW, Major PW, Carey JP. Analytically determined mechanical properties of, and models for the periodontal ligament: critical review of literature. J Biomech. 2012;45(1):9-16.
15. Martinez Choy SE, Lenz J, Schweizerhof K, Schmitter M, Schindler HJ. Realistic kinetic loading of the jaw system during single chewing cycles: a finite element study. J Oral Rehabil. 2017;44(5):375-84.
16. Jing Y, Han X, Cheng B, Bai D. Three-dimensional FEM analysis of stress distribution in dynamic maxillary canine movement. Chinese Science Bulletin. 2013;58(20):2454-9.
17. Qian Y, Fan Y, Liu Z, Zhang M. Numerical simulation of tooth movement in a therapy period. Clin Biomech (Bristol, Avon). 2008;23 Suppl 1:S48-52.
18. Cai Y, Yang X, He B, Yao J. Finite element method analysis of the periodontal ligament in mandibular canine movement with transparent tooth correction treatment. BMC Oral Health. 2015;15(1):106.
19. Serio FG, Hawley CE. Periodontal trauma and mobility. Diagnosis and treatment planning. Dent Clin North Am. 1999;43(1):37-44.
20. Geramy A, Faghihi S. Secondary trauma from occlusion: three-dimensional analysis using the finite element method. Quintessence Int. 2004;35(10):835-43.
21. Wang CH, Liu HW, Ou KL, Teng NC, Yu JJ, Huang HM. Natural frequency analysis of tooth stability under various simulated types and degrees of alveolar vertical bone loss. Proc Inst Mech Eng H. 2008;222(6):983-9.
22. Wang H, Wu JY, Zhou Q, Liu J. [Initial stress in the periodontal membrane of maxillary first molar with different alveolar bone height by intrusion: 3-dimensional finite element analysis]. Shanghai Kou Qiang Yi Xue. 2013;22(3):247-51.

23. Ona M, Wakabayashi N. Influence of alveolar support on stress in periodontal structures. J Dent Res. 2006;85(12):1087-91.
24. Chachada AD, Hazarey PV, Aley MS, Atram HK, Kharche A. Effect of Three-wall Bony Defect along Various Root Surfaces on Position of Center of Resistance: A 3D Finite Element Analysis. J Contemp Dent Pract. 2015;16(8):688-91.
25. Agarwal A, Mahajan S, Verma S, Bhardwaj P, Sharma G. Evaluation of the Stress Induced in Tooth, Periodontal Ligament & Alveolar Bone with Varying Degrees of Bone Loss During Various Types of Orthodontic Tooth Movements. J Clin Diagn Res. 2016;10(2):ZC46-52.
26. Cobo J, Sicilia A, Arguelles J, Suarez D, Vijande M. Initial stress induced in periodontal tissue with diverse degrees of bone loss by an orthodontic force: tridimensional analysis by means of the finite element method. Am J Orthod Dentofacial Orthop. 1993;104(5):448-54.
27. Choy K, Pae EK, Park Y, Kim KH, Burstone CJ. Effect of root and bone morphology on the stress distribution in the periodontal ligament. Am J Orthod Dentofacial Orthop. 2000;117(1):98-105.
28. Geramy A. Initial stress produced in the periodontal membrane by orthodontic loads in the presence of varying loss of alveolar bone: a three-dimensional finite element analysis. Eur J Orthod. 2002;24(1):21-33.
29. Jeon PD, Turley PK, Ting K. Three-dimensional finite element analysis of stress in the periodontal ligament of the maxillary first molar with simulated bone loss. Am J Orthod Dentofacial Orthop. 2001;119(5):498-504.
30. Dannan A. An update on periodontic-orthodontic interrelationships. J Indian Soc Periodontol. 2010;14(1):66-71.
31. Kondo T, Wakabayashi N. Influence of molar support loss on stress and strain in premolar periodontium: a patient-specific FEM study. J Dent. 2009;37(7):541-8.
32. Svanberg G. Influence of trauma from occlusion on the periodontium of dogs with normal or inflamed gingivae. Odontol Revy. 1974;25(2):165-78.
33. Ericsson I, Lindhe J. Effect of longstanding jiggling on experimental marginal periodontitis in the beagle dog. J Clin Periodontol. 1982;9(6):497-503.
34. Lindhe J, Svanberg G. Influence of trauma from occlusion on progression of experimental periodontitis in the beagle dog. J Clin Periodontol. 1974;1(1):3-14.
35. Nyman S, Lindhe J, Ericsson I. The effect of progressive tooth mobility on destructive periodontitis in the dog. J Clin Periodontol. 1978;5(3):213-25.
36. Burgett FG, Ramfjord SP, Nissle RR, Morrison EC, Charbeneau TD, Caffesse RG. A randomized trial of occlusal adjustment in the treatment of periodontitis patients. J Clin Periodontol. 1992;19(6):381-7.
37. Shillingburg. HT, Boyd DR. FUNDAMENTALS OF FIXED PROSTHODONTICS. 4 ed: Quintessence Publishing Co, Inc; 2012.
38. Borchers L, Reichart P. Three-dimensional stress distribution around a dental implant at different stages of interface development. J Dent Res. 1983;62(2):155-9.